IEEE Access
Multidisciplinary | Rapid Review | Open Access Journal

Received May 11, 2020, accepted June 2, 2020, date of publication July 3, 2020, date of current version August 4, 2020.

Digital Object Identifier 10.1109/ACCESS.2020.3006992

A Head/Taillight Featuring Hybrid Planar Visible Light Communications/Millimetre Wave Antenna for Vehicular Communications

MOJTABA MANSOUR ABADI[1], (Member, IEEE), PAVEL HAZDRA[2], (Member, IEEE), JAN BOHATA[2], (Member, IEEE), PETR CHVOJKA[2], PAUL ANTHONY HAIGH[3], (Member, IEEE), ZABIH GHASSEMLOOY[1], (Senior Member, IEEE), AND STANISLAV ZVANOVEC[2], (Senior Member, IEEE)

[1]Optical Communications Research Group, Department of Mathematics, Physics and Electrical Engineering, Northumbria University, Newcastle upon Tyne NE1 8ST, U.K.
[2]Department of Electromagnetic Field, Faculty of Electrical Engineering, Czech Technical University in Prague, 16627 Prague, Czech Republic
[3]Intelligent Sensing and Communications Group, School of Engineering, Newcastle University, Newcastle upon Tyne NE1 7RU, U.K.

Corresponding author: Mojtaba Mansour Abadi (mojtaba.mansour@northumbria.ac.uk)

This work was supported in part by the UKEPSRC under Grant EP/P006280/1: Multifunctional Polymer Light-Emitting Diodes with Visible Light Communications (MARVEL), and in part by the Horizon 2020 MSCITN under Grant 764461 (VISION).

ABSTRACT With the emergence of the fifth generation and beyond mobile networks, both visible light communications (VLC) and radio frequency (RF) or millimetre wave (mmW) systems are expected to maintain the connectivity in various environments. In outdoor environments the link (VLC or RF) availability is paramount, which is affected by channel conditions. In particular, in vehicular communications other vehicles, harsh environment, and road geometry and structure will have the impact on the link connectivity and availability. In such cases, a front-end antenna solution, which benefits both optical and RF communication links, can be seen as an attractive option that can be fitted in future vehicles. In this paper, we present the design and practical implementation of a planar hybrid VLC/mmW antenna operating at 20.8 GHz and show measured results for characterization of RF and VLC links as well as communications performance. We have used the widely adopted on-off keying and quadrature amplitude modulation schemes with different orders to demonstrate data rates of 5 Mb/s and up to 100 Mb/s for the VLC and mmW links, respectively. By measuring the bit error rate and the error vector magnitude for VLC and RF links, respectively for each modulation we have shown that the proposed hybrid planar antenna is suitable for example in a typical vehicle-to-vehicle communications.

INDEX TERMS VLC, mmW, hybrid VLC/mmW, hybrid VLC/RF, hybrid antenna.

I. INTRODUCTION

Hybrid optical-radio frequency wireless technologies are an attractive solution for reliable outdoor communication links. They ensure reliability in all weather conditions whilst simultaneously relieving the pressure on radio frequency (RF) spectral usage at low cost and low complexity [1], [2]. As a result, optical/RF hybrid systems have become the focus of ever-increasing attention in recent years. A number of experimental demonstrations have shown improved reliability and reduced system outage [3], higher throughput [4] and lower power consumption [3]. Improved technological integration has also been demonstrated through advances in both soft [5], hard [6] and neural [7], [8] based switching modes between each transmission media [9].

The associate editor coordinating the review of this manuscript and approving it for publication was Xueqin Jiang.

Hybrid systems can broadly be classified as optical or RF, both of which have undergone substantial developments over the previous decades. For optical links, either infrared or visible light bands may be used to offer free space optics (FSO) and visible light communications (VLC), respectively. The advantages of FSO include high bandwidths and low power consumption [10], however, it is subject to eye safety conditions, which impose an upper limit on the optical transmit power. Therefore, VLC has become an attractive option in hybrid systems as it offers high power and bandwidth but with relaxed eye safety requirements. This comes at the cost of a less focused beam, which restricts the transmission distances. Note, using a laser with white light, the transmission distance can be increased further. On the other hand, the RF component has a high degree of customisability such as the power, directionality, beamform and carrier frequency, amongst others. In recent years, due to the overcrowding of the RF

spectrum, research interests have shifted towards higher carrier frequencies with major focus on millimetre (mmW) technology for the fifth generation and beyond wireless networks. Note that, all hybrid systems fall into three main fundamental categories in terms of the link loads: (*i*) parallel transmission, where both links are transmitting the same data at the same rate; (*ii*) a dominant link transmission, where the faster and slower links are selected as the default and backup, respectively, and the communications system has to adopt the speed based on the active link; and (*iii*) dual transmission links with different data loads depending on the channel conditions [10].

There are several key applications where the motivation to use a hybrid antenna for both indoor and outdoor applications is clear. For indoor scenarios, femtocell wireless access is attractive, while for outdoor applications front/backhauling is also of an interest [11]. One outdoor application that takes advantage of both VLC and mmW technologies is the vehicular communications. In such networks, the VLC transmitters (Txs) can easily be integrated into vehicle's light-emitting diodes (LEDs)-based head- and tail-lights [12] while the highly directional and high frequency mmW link can result in much reduced inter-channel interference.

To the best of authors' knowledge, no feasible solution has been proposed so far which integrates a hybrid front-end antenna including VLC (with illumination) and mmW in a single package. In addition, the antenna should comply with the three possible hybrid transmission configurations outlined above. Therefore, in this work, we design and experimentally demonstrate a hybrid VLC/planar mmW antenna for an application in vehicular communications networks. The proposed antenna can be used within vehicle's head/tail-lights to provide illumination and data communications simultaneously. The developed VLC transceiver consists of 6 high power white LEDs and two photodiodes (PDs). The planar mmW antenna operates at 20.8 GHz using linear polarisation. Note that, the proposed design procedure is easily transferable to mmW frequencies above 30 GHz so as general we refer it as the mmW design, which can be used in future mmW-based systems. We have adopted quadrature amplitude modulation (QAM) and on-off keying (OOK) for the mmW and VLC links, respectively. This results in less complex modulation and coding schemes but on the other hand reduces the overall system cost-effectiveness and power efficiency. We demonstrate that, links up to 50 Mbaud and 5 Mbps can be realized for the hybrid mmW and VLC links, respectively.

The rest of the paper is organized as follows; Section II with subsections on mmW and VLC describe the structure of the hybrid antenna. Section III discusses the hybrid antenna fabrication, design and the system deployment alongside experimental measurements and performance evaluation. The conclusion is drawn in Section IV.

II. HYBRID ANTENNA STRUCTURE

A. THE mmW COMPONENT

The mmW antenna was designed using the CST Microwave Studio [13]. It consists of a four-element microstrip array

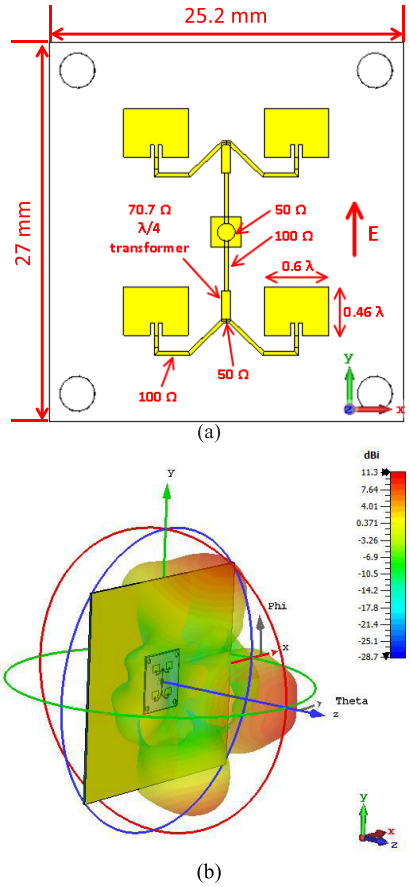

FIGURE 1. (a) Patch antenna diagram showing the dimensions and electric field polarisation. (b) 3D electromagnetic model of the antenna embedded into the board represented by metal and its radiation pattern.

printed on a 0.5 mm thick Rogers RO4350B substrate with a 25 × 27 mm^2 antenna printed circuit board (PCB). Note, there is no particular rule for the number of elements in the array antenna. Here, we have adopted a four-element array because of size consideration. The basic radiating element is an inset-fed microstrip antenna with an input impedance of 100 Ω. Note, more on the design of inset-fed can be found in [14], [15]. The two antennas are connected in parallel, yielding 50 Ω, which is transformed via a λ/4 transformer with an impedance $Z_{tr} = \sqrt{100 \times 50} = 70.7\Omega$ back to 100 Ω. The same is done for the second pair of antennas, resulting in 2 × 100 Ω in parallel at the centre feeding point, see Fig. 1(a). A detailed schematic of the coupling network is presented in Appendix. Fig. 1(b) shows the 3D electromagnetic model of the antenna embedded into the board represented by the metal and its radiation pattern. This figure gives the reader a better idea about how the radiation pattern will look like in manufactured products. The operating frequency is 20.8 GHz with respect to the manufacturing tolerances. A similar approach with different (smaller) connectors and substrate could be adopted and optimised for higher frequency bands if desirable.

B. THE VLC COMPONENT

The VLC Tx circuit is based on a transistor switch circuit with two pairs of three LEDs. A buffer is used to

TABLE 1. Fabricated hybrid antenna parameters.

Part	Parameter	Value
VLC	Base resistor	1.41 kΩ
	Emitter resistor	70 Ω
	Decoupling capacitor	220 pF
	Switching transistor	On Semi BSR14
	Photodiode	Centronic OSD15-5T
	LED	Cree 4V white LED
	TIA	Analog Devices AD8015ARZ
mmW	PCB size	25 × 27 mm
	PCB type	0.5 mm thick Rogers RO4350B
	Patch size	4.60 × 3.45 mm^2

match the data source and the Tx's input impedances. The used white LEDs (Cree C503C-WAN-CCADB231) have a bandwidth of 1.69 MHz. The measured voltage-current (VI) and illuminance-current (LI) characteristics of the LEDs are depicted in Fig. 2. The values of base and emitter resistors are selected to ensure that the transistor is switched between the off and saturated states based on the input signal. The saturation current of the LED is set to 70 mA. Decoupling capacitors are used to isolate both the Tx and the receiver (Rx) from the supply lines to reduces the crosstalk. The optical Rx is composed of a standard PD (Centronics OSD15-5T) and a transimpedance amplifier (TIA, Analog Devices AD8015ARZ). The generated photocurrent is converted into an amplified differential voltage signal prior to low-pass filtering (∼10 MHz cut-off frequency) for limiting the out-of-band noise. All VLC circuits were manufactured on FR4. The circuit diagrams as well as details of used components are presented in Appendix. More information and design guidelines for VLC transceivers are available in [16]–[20].

The key parameters for both the mmW and VLC components are highlighted in Table 1. The VLC section was first simulated using Analog Devices LTspice XVII [21] to verify the circuit functionality and the PCB was designed by KiCAD EDA package version 5 [22]. A photograph of the integrated hybrid antenna is shown in Fig. 3 with the key components highlighted as well as antenna size.

III. RESULTS AND DISCUSSION

A. MEASUREMENT OF THE mmW ANTENNA

The normalised simulated and measured radiation patterns and the matching of the mmW antenna are shown in Fig. 4, where a very close agreement can be observed. Note that, the side-lobes in the E-plane have a higher magnitude than those in the H-plane, which is attributed to the surface waves in the substrate. However, the side-lobes can be reduced by various means, e.g., (*i*) decreasing the thickness of the substrate; (*ii*) reducing the relative permittivity of the substrate; or (*iii*) adding a metallic rim around the antenna [23], [24].

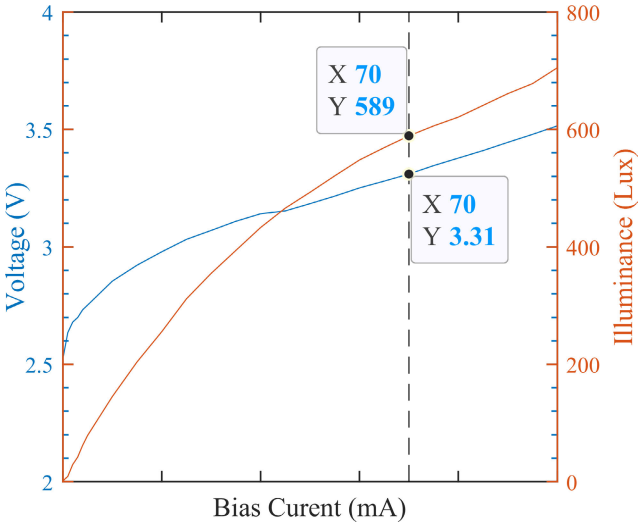

FIGURE 2. VI and LI plots of the used LED. The selected LED's bias points are marked on the plots.

However, the downside will be the mechanical stability, the fabrication cost and complexity of the antenna. Note that, for the main lobe the simulated and measured gains are 11.8 and 10.5 dBi, respectively at the 20.8 GHz operating frequency. Note that, the simulated cross polarization result shows a low level (i.e., < -40 dB) along broadside direction.

As shown in Fig. 4(b), the measured centre operating frequency is 20.8 GHz with a relative −10 dB bandwidth of 3.3% (note, the simulated bandwidth is 3%). The marginal differences are attributed to the manufacturing tolerances of the components used and the fact that the catalogue value was used for the substrate permittivity in simulations. Finally, the simulation model depicted in Fig. 1(b) shows the embedded microstrip antenna in a simplified model of the overall hybrid board. Clearly, the metal surface of the VLC board has a negligible impact on the antenna array and its performance.

To properly evaluate the fabricated hybrid antenna in a real communications system, we carried out two sets of measurements. The 1st and 2nd set of measurements were focused on the performance (i.e., bandwidth and crosstalk) of the mmW and VLC links in parallel, in a laboratory-controlled environment mimicking an outdoor vehicle-to-vehicle communication, respectively. The 802.11p defined channel does not apply here since the standard defines channels at 5.9 GHz due to the short transmission link length of 2 m, which is a typical distance between vehicles in urban areas. In such cases, the line-of-sight is considered to be the dominant transmission path for both VLC and mmW links.

B. VLC LINK

Here, we have used two hybrid antennas spaced apart by 50 cm and measured the Q-factor of the received signal at one antenna at a data rate of 10 Mbps under a dark environment. The measured Q-factor as a function of the data rate for a single and multiple LEDs is depicted in Fig. 5(a) along with the horizontal lines equivalent to the Q-factor for the

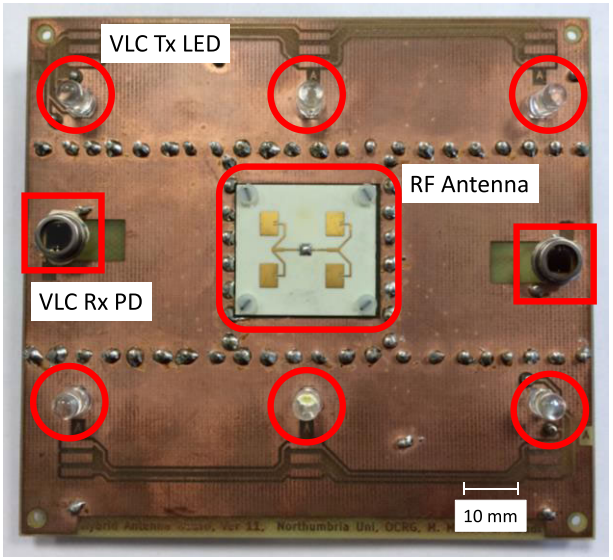

(a)

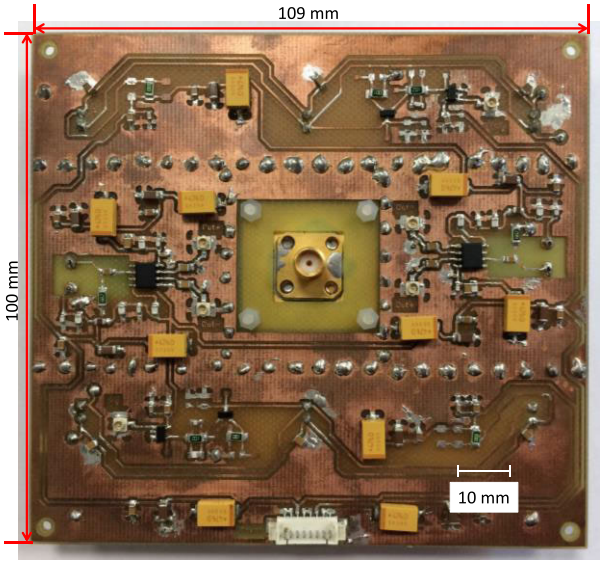

(b)

FIGURE 3. Fabricated hybrid VLC/mmW antenna: (a) front side and (b) back side. Circle and rectangle show LEDs and PDs, respectively.

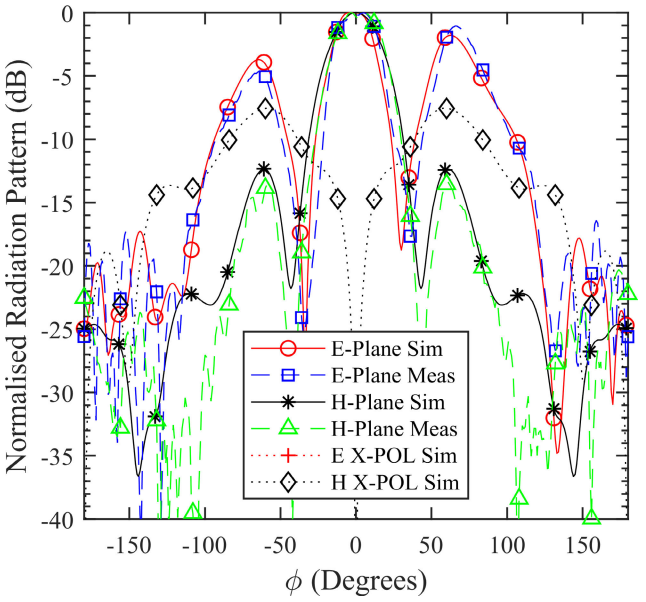

(a)

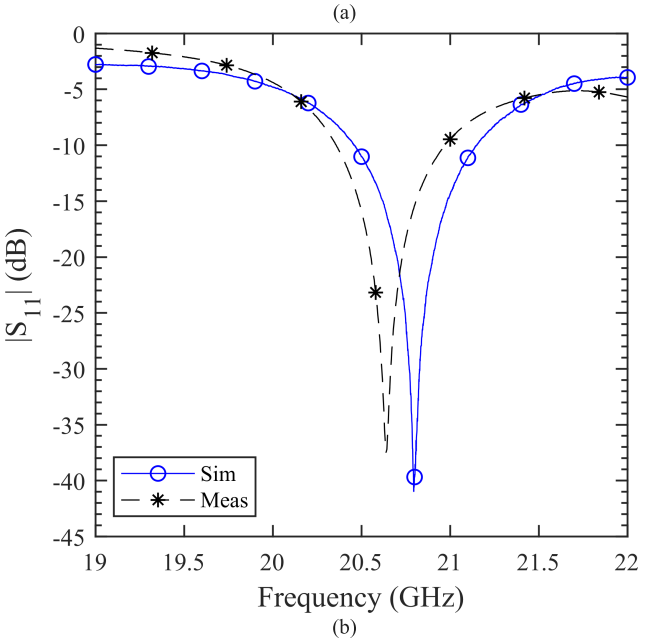

(b)

FIGURE 4. Simulation and measurements for the mmW part (Section III.A: Measurement of the mmW antenna): (a) the radiation pattern for E and H planes. Cross polarization in the E-plane is < -80 dB and is not visible in the graph; and (b) the matching (simulated and measured) for the fabricated hybrid antenna.

BER values of 3.8×10^{-3} (i.e., the forward error correction BER limit) and 10^{-6}. Due to the short distance (i.e., 105 mm) between the LEDs mounted on the PCB, the maximum phase difference between the received signals from any LEDs at a data rate of 10 Mbps is $\sim 1.3^{\circ}$, which is small and thus can be neglected. As shown in Fig. 5(a), the maximum relative difference between the Q-factor of one LED and multiple LEDs is 30%. In another test, we carried out an experiment for the link where the VLC Tx of one antenna was fed by a random OOK signal while the Rx was receiving a signal from a separate light source. We carried out the measurement with and without the low pass filter (LPF) for the data rate in the range of 1 to 10 Mbps, see Fig. 5(b). What we observed was that, for the case with no LPF, the sudden switch toggle of the Tx resulted in power line voltage drop. On the other hand, the Rx circuit with a feedbacked amplifier stage (e.g., the TIA section) is affected by this supply voltage drop, thus resulting in a damped ringing signal with the frequency of 78.8 MHz embedded in the output of TIA. This unwanted signal coupling can be removed by fabricating the circuit on multilayers PCBs with dedicated power planes, decoupling capacitors on the power lines and power pins of the components. However, since the ringing frequency is out of the VLC/mmW signal frequency range, we simply used an LPF at the output of the TIA. Note that, using the via stitching technique on the PCB we have increased the isolation between the Tx and the Rx sections.

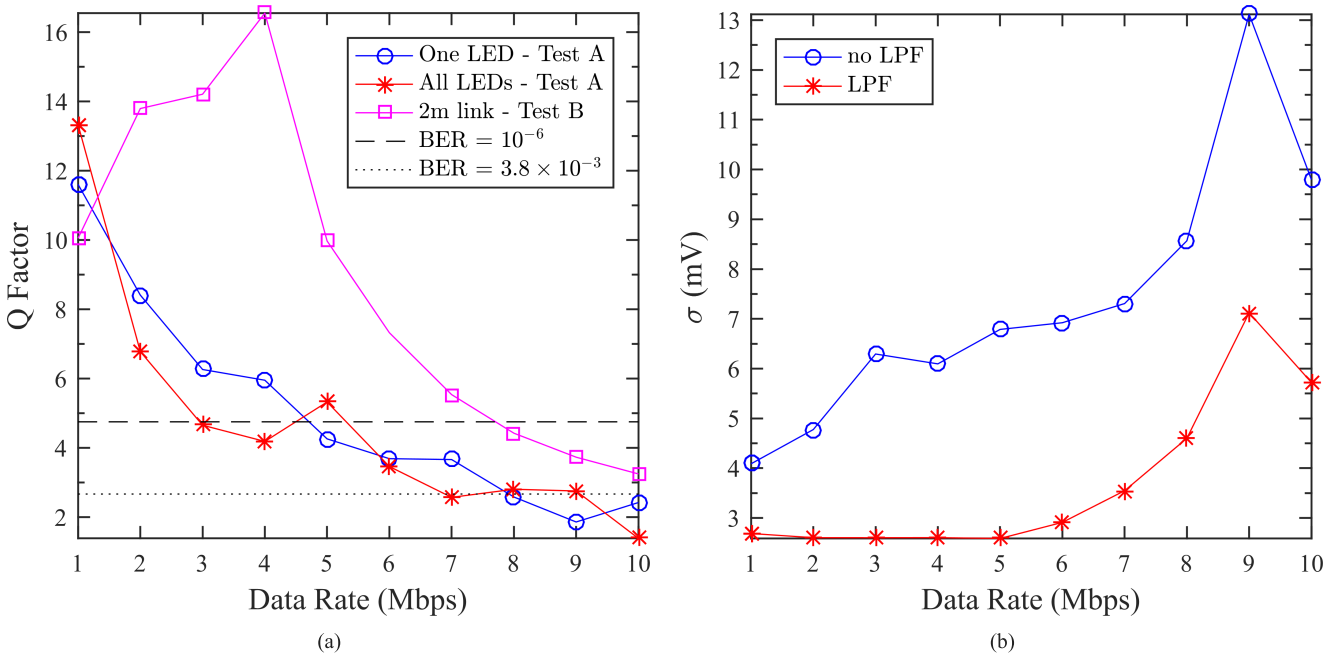

FIGURE 5. (a) The Q-factor as a function of the data rate for the hybrid antenna with a single LED and all LEDs (Section III.B: VLC test) and for the BER values of 3.8×10^{-3} and 10^{-6}. Also shown is the performance of VLC Tx over a 2 m link (Section III.C: hybrid VLC/MMW antenna implementation in a real system). (b) Standard deviation versus the data rate for theRx output voltage before and after LPF (Section III.B: VLC test).

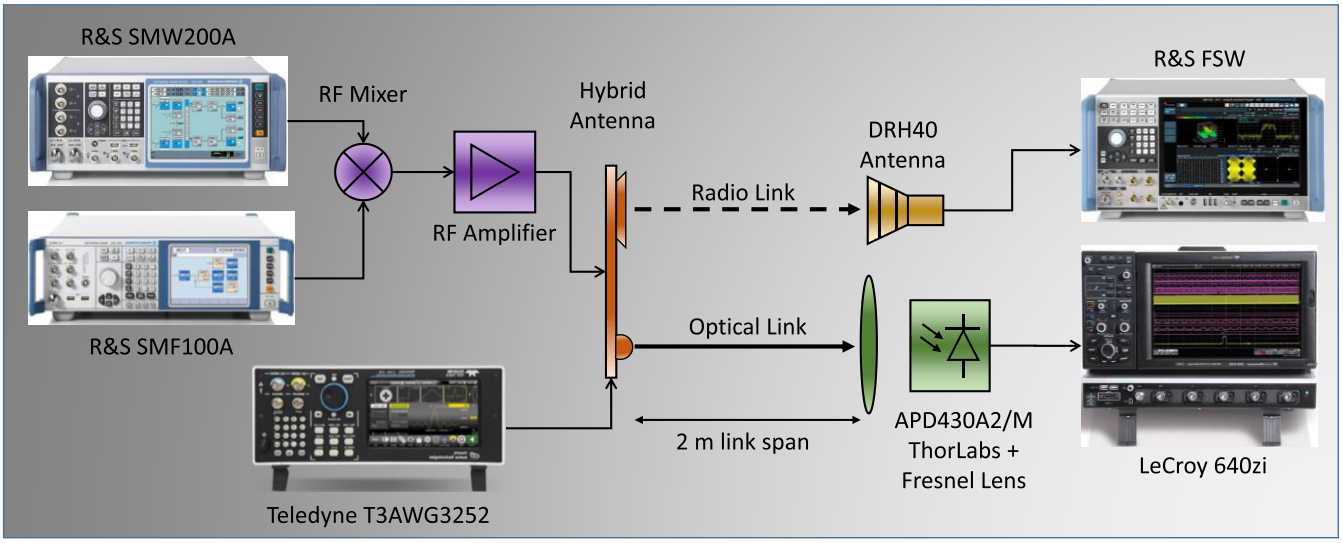

FIGURE 6. A block diagram of the experimental setup for the hybrid VLC/mmW antenna under the real system test environment.

C. HYBRID VLC/mmW ANTENNA IMPLEMENTATION IN A REAL SYSTEM

Finally, we carried out measurements for both links being active over a 2 m long transmission link using the block diagram illustrated in Fig. 6. The VLC Tx was fed with a 10^5 bit long pseudorandom binary sequence (PRBS) signal using a waveform generator (Teledyne T3AWG3252). In order to properly quantify the Tx performance, the VLC Rx included a Fresnel lens (diameter and focal length of 63 mm and 6.6 mm, respectively) and an optical Rx (Thorlabs APD430A2/M). The electrical signal was captured using a real-time sampling storage scope (LeCroy Waverunner 640Zi) for further offline processing. Here, we also measured the Q-factor of the received signal for a range of data rates, see the purple curve in Fig. 5(a). For the 2 m case, we notice an unexpected peak in the plot, which is simply caused by frequency response of the optical Rx. The optical Rx has a low cut-off frequency acting as a high pass filter, thus the increase of the Q-factor for frequencies below 4 MHz. However, as frequency increases the LED frequency response become the dominant factor, which leads to deterioration of the circuit performance. The peak at around 3 to 4 MHz is expected, which coincide with the frequency range of the white LED.

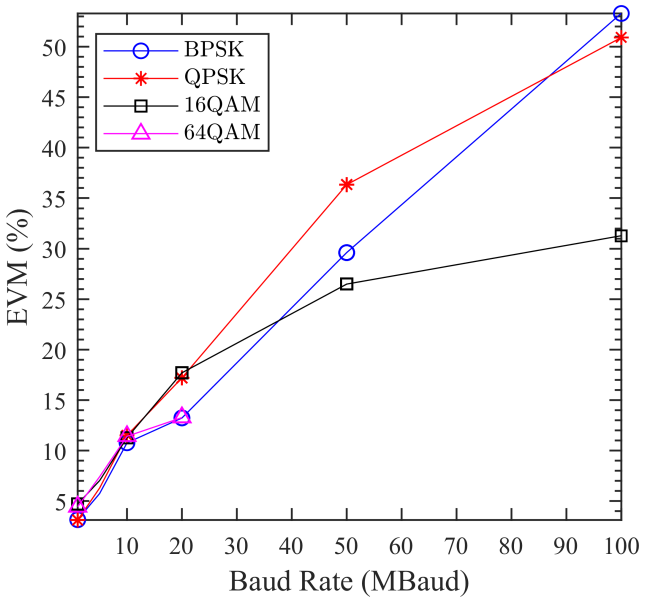

FIGURE 7. Measured EVM of mmW link over 2 m experimental setup for different digital mmodulation schemes link (Section III.C: hybrid VLC/mmW antenna implementation in a real system).

As for the mmW section, the antenna was fed by a 20.8 GHz RF signal. Here, binary phase shift keying (BPSK), quadrature phase shift keying (QPSK), 16- and 64-QAM at the symbol rates in the range of 1 to 100 Mbaud were used. The signals were generated using a signal generator (R&S SMW200A), and then up-converted to the desired frequency using a mixer and carrier generator (R&S SMF100A) followed by amplification using a low-noise RF amplifier (Analog Devices HMC1131). Similar to the VLC section, to appropriately qualify the antenna performance, a double ridged horn antenna (DRH40 – RFspin, s.r.o.) with a gain of 14 dBi at 20.8 GHz was used at the Rx. The evaluation of the received signal in terms of the received electrical power and the error vector magnitude (EVM) using a signal analyser (R&S FSW) is illustrated in Fig. 7. As can be observed, with

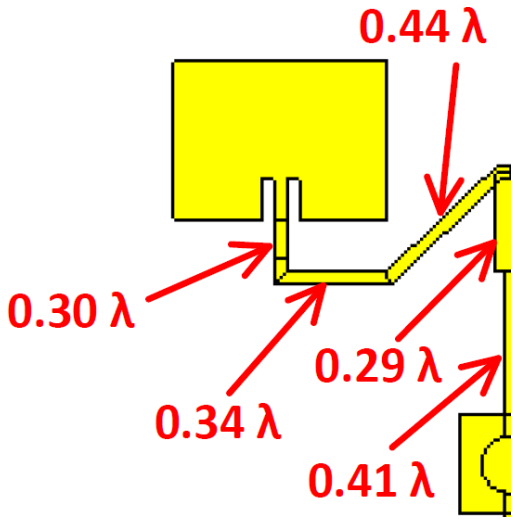

FIGURE 8. Detailed diagram of the coupling network of RF antenna.

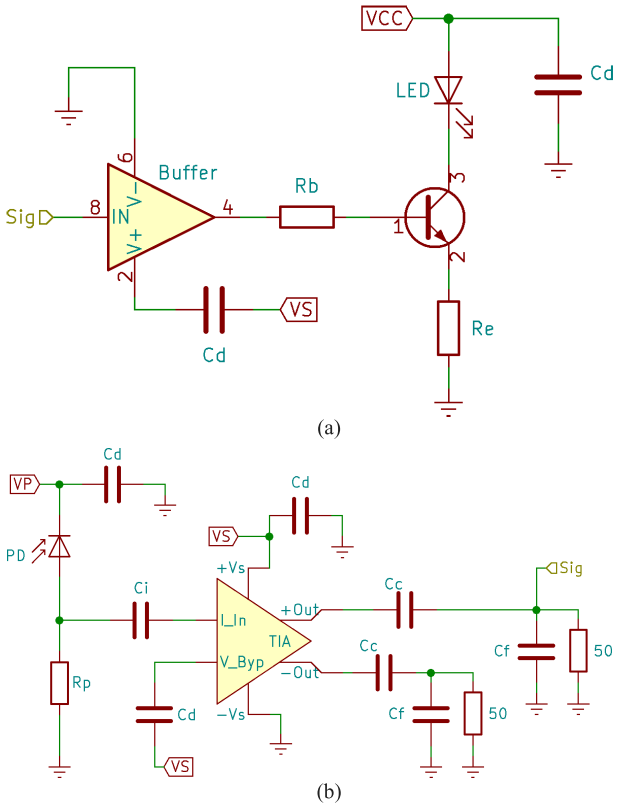

FIGURE 9. a) Tx switching circuit blockdiagram, and b) Rx transimpedance amplifier (TIA) circuit blockdiagram.

no equalisation and using multi-level modulation techniques, the hybrid antenna offers the minimum data rates of 5 Mbps and 50 Mbaud for VLC and mmW, respectively, which is sufficient for low-data rates applications such as vehicular communications. Moreover, our investigation demonstrated the operation of the proposed hybrid antenna for the following cases: (*i*) parallel transmission of VLC and mmW at a data rate of 5 Mbps; (*ii*) mmW and VLC serving as the default and backup links with data rates of 50 Mbaud and 5 Mbps, respectively; and (*iii*) mmW and VLC operating depending on the channel conditions, where for a clear channel the data rate could exceed 50 Mbaud.

IV. CONCLUSION

We proposed a hybrid VLC/mmW antenna featuring illumination, and data transmission for use in vehicular communications. The paper outlined the new design of mmW antenna and the supporting Tx and Rx circuits for VLC. First, we assessed the characteristics of VLC and mmW sections individually and then evaluated the performance of the proposed antenna in a mimicked real scenario by measuring the Q-factor and the EVM for VLC and mmW links, respectively. The results showed that, the minimum data rates of 5 Mbps and 50 Mbaud for VLC and mmW, respectively are perfectly achievable. Our measurement showed that, a BER of 10^{-6} and an acceptable EVM value for VLC and mmW links for each modulation scheme, respectively. Therefore, we showed that the proposed hybrid antenna can provide reliable VLC

TABLE 2. Fabricated VLC transceiver parameters.

Parameter	Value
R_b	1.41 kΩ
R_e	70 Ω
R_p	7 kΩ
C_d	220 pF
C_i	10 nF
C_c	47 µF
Buffer	NC7SZ08M5X
Transistor	BSR14
Photodiode	OSD15-5T
LED	Cree 4V white LED
TIA	AD8015ARZ
VS	+5 V
VP	+12 V

and mmW links (i.e., illumination and data transmission) in future vehicular communications.

APPENDIX

RF ANTENNA

The detailed dimensions of the coupling network from Fig. 1(a) is presented in Fig. 8.

VLC TRANSCEIVER

Fig. 9 shows the circuit diagram of the VLC Tx and Rx while Table 2 summarises the used components values.

ACKNOWLEDGMENT

This work was gratefully supported by the UKEPSRC grant EP/P006280/1: Multifunctional Polymer Light-Emitting Diodes with Visible Light Communications (MARVEL) and the Horizon 2020 MSCITN grant 764461 (VISION).

REFERENCES

[1] B. Bag, A. Das, I. S. Ansari, A. Prokes, C. Bose, and A. Chandra, "Performance analysis of hybrid FSO systems using FSO/RF-FSO link adaptation," *IEEE Photon. J.*, vol. 10, no. 3, pp. 1–17, Jun. 2018.

[2] S. Enayati and H. Saeedi, "Deployment of hybrid FSO/RF links in backhaul of relay-based rural area cellular networks: Advantages and performance analysis," *IEEE Commun. Lett.*, vol. 20, no. 9, pp. 1824–1827, Sep. 2016.

[3] J. Kong, M. Ismail, E. Serpedin, and K. A. Qaraqe, "Energy efficient optimization of base station intensities for hybrid RF/VLC networks," *IEEE Trans. Wireless Commun.*, vol. 18, no. 8, pp. 4171–4183, Aug. 2019.

[4] D. A. Basnayaka and H. Haas, "Hybrid RF and VLC systems: Improving user data rate performance of VLC systems," in *Proc. IEEE 81st Veh. Technol. Conf. (VTC Spring)*, May 2015, pp. 1–5.

[5] K. O. Odeyemi and P. A. Owolawi, "Selection combining hybrid FSO/RF systems over generalized induced-fading channels," *Opt. Commun.*, vol. 433, pp. 159–167, Feb. 2019.

[6] F. Nadeem, M. Loeschnig, B. Geiger, G. Kandus, E. Leitgeb, and S. S. Muhammad, "Comparison of link selection algorithms for free space optics/radio frequency hybrid network," *IET Commun.*, vol. 5, no. 18, pp. 2751–2759, Dec. 2011.

[7] A. A. B. Raj, J. A. V. Selvi, and S. Durairaj, "Comparison of different models for ground-level atmospheric turbulence strength (C_n^2) prediction with a new model according to local weather data for FSO applications," *Appl. Opt.*, vol. 54, no. 4, pp. 802–815, 2015.

[8] J. Tóth, L'. Ovseník, J. Turán, L. Michaeli, and M. Márton, "Classification prediction analysis of RSSI parameter in hard switching process for FSO/RF systems," *Measurement*, vol. 116, pp. 602–610, Feb. 2018.

[9] M. Najla, P. Mach, Z. Becvar, P. Chvojka, and S. Zvanovec, "Efficient exploitation of radio frequency and visible light communication bands for D2D in mobile networks," *IEEE Access*, vol. 7, pp. 168922–168933, 2019.

[10] M. M. Abadi, Z. Ghassemlooy, S. Zvanovec, M. R. Bhatnagar, and Y. Wu, "Hard switching in hybrid FSO/RF link: Investigating data rate and link availability," in *Proc. IEEE Int. Conf. Commun. Workshops (ICC Workshops)*, May 2017, pp. 463–468.

[11] M. B. Rahaim and T. D. C. Little, "Toward practical integration of dual-use VLC within 5G networks," *IEEE Wireless Commun.*, vol. 22, no. 4, pp. 97–103, Aug. 2015.

[12] B. Turan, O. Narmanlioglu, S. C. Ergen, and M. Uysal, "Physical layer implementation of standard compliant vehicular VLC," in *Proc. IEEE 84th Veh. Technol. Conf. (VTC-Fall)*, Sep. 2016, pp. 1–5.

[13] (Nov. 21, 2019). *CST Microwave Studio*. https://www.3ds.com/products-services/simulia/products/cst-studio-suite/electromagnetic-systems/

[14] P. Sharma, S. K. Koul, and S. Chandra, "Micromachined inset-fed patch antenna at Ka-band," in *Proc. Asia–Pacific Microw. Conf.*, Dec. 2006, pp. 693–696.

[15] Y. Hu, D. R. Jackson, J. T. Williams, and S. A. Long, "A design approach for inset-fed rectangular microstrip antennas," in *Proc. IEEE Antennas Propag. Soc. Int. Symp.*, 2006, pp. 1491–1494.

[16] K. Modepalli and L. Parsa, "Lighting up with a dual-purpose driver: A viable option for a light-emitting diode driver for visible light communication," *IEEE Ind. Appl. Mag.*, vol. 23, no. 2, pp. 51–61, Mar. 2017.

[17] K. Modepalli and L. Parsa, "Dual-purpose offline LED driver for illumination and visible light communication," *IEEE Trans. Ind. Appl.*, vol. 51, no. 1, pp. 406–419, Jan. 2015.

[18] T. Kishi, H. Tanaka, Y. Umeda, and O. Takyu, "A high-speed LED driver that sweeps out the remaining carriers for visible light communications," *J. Lightw. Technol.*, vol. 32, no. 2, pp. 239–249, Jan. 15, 2014.

[19] P. Horowitz and W. Hill, *The Art of Electronics*. Cambridge, U.K.: Cambridge Univ. Press, 1989.

[20] F. Che, L. Wu, B. Hussain, X. Li, and C. P. Yue, "A fully integrated IEEE 802.15.7 visible light communication transmitter with on-chip 8-W 85% efficiency boost LED driver," *J. Lightw. Technol.*, vol. 34, no. 10, pp. 2419–2430, May 15, 2016.

[21] (Nov. 21, 2019). *LTspice*. [Online]. Available: https://www.analog.com/en/design-center/design-tools-and-calculators/ltspice-simulator.html

[22] (Nov. 21, 2019). *KiCad EDA*. [Online]. Available: http://www.kicad-pcb.org/

[23] D. M. Pozar, *Microwave Engineering*, 2nd ed. New York, NY, USA: Wiley, 1998.

[24] M. T. Nguyen, B. Kim, H. Choo, and I. Park, "Effects of a cavity structure on a half E-shaped microstrip patch antenna," in *Proc. Int. Workshop Antenna Technol. (iWAT)*, Mar. 2011, pp. 310–313.

MOJTABA MANSOUR ABADI (Member, IEEE) received the B.Sc. degree in electrical engineering from Islamic Azad University, Fasa, Iran, in 2005, the M.Sc. degree in electromagnetic fields and waves from the K.N. Toosi University of Technology, Tehran, Iran, in 2008, and the Ph.D. degree in optical communication from the Optical Communication Research Group (OCRG), Northumbria University, Newcastle upon Tyne, U.K., in 2016. His research subject was hybrid free-space optical (FSO)/radio frequency (RF) communication systems, particularly hybrid antennas. He also developed differential signaling technique for mitigating channel effects in FSO links. From 2017 to 2018, he was as a Research Assistant with the School of Engineering, University of Glasgow, Glasgow, Scotland. He worked on high capacity FSO system using space division multiplexing (SDM), autonomous FSO alignment systems, as well as 1 Gbps underwater optical wireless communications. Since July 2018, he returned to OCRG as a Researcher to work on high-speed ground to train FSO link. Since May 2020, he has joined the Mathematics, Physics and Electrical Engineering (MPEE) Department, Northumbria University, as a Lecturer.

PAVEL HAZDRA (Member, IEEE) was born in Prague, Czech Republic, in 1977. He received the M.Sc. and Ph.D. degrees in electrical engineering from the Czech Technical University in Prague, in 2003 and 2009, respectively. Since 2012, he has been an Associate Professor with the Department of Electromagnetic Field, CTU in Prague. He has authored or coauthored more than 50 journal and conference papers. His research interests are in the area of EM/antenna theory, electrically small antennas, reflector antennas, and their feeds and antennas for amater radio purposes.

JAN BOHATA (Member, IEEE) was born in Prague, Czech Republic, in 1988. He received the B.S. and M.S. degrees in communications, electronics, and multimedia from the Faculty of Electrical Engineering, Czech Technical University in Prague, in 2012, and the Ph.D. degree in radio electronics in 2018. In 2012, he joined the Wireless and Fiber Optics Group, Department of Electromagnetic Field with a main focus on microwave photonics, fiber and free space optics networks, and optical communications in harsh environments. He is the author of more than 30 journal and conference papers and involved in a number of national and European research projects. He is a member of OSA.

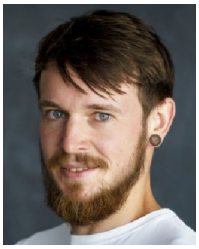

PETR CHVOJKA received the M.Sc. and Ph.D. degrees from the Faculty of Electrical Engineering, Czech Technical University (CTU) in Prague, in 2013 and 2018, respectively. He currently works as a Research Fellow at the Department of Electromagnetic Field, CTU in Prague, where he is also a member of the Wireless and Fiber Optics Group. His research focuses on optical systems design and modeling, including inorganic and organic devices and digital signal processing techniques for visible light communications. During his research, he has been involved in several European (VisIoN, COST OPTICSWISE) and Czech scientific projects (RAINBOWS) and was on internships at University College London, London, U.K., Northumbria University, Newcastle upon Tyne, U.K., and Ben-Gurion University of Negev, Beersheba, Israel.

PAUL ANTHONY HAIGH (Member, IEEE) received the B.Eng. and Ph.D. degrees from Northumbria University, Newcastle upon Tyne, U.K., in 2010 and 2014, respectively. He has been a Lecturer in communication with Newcastle University, U.K., since March 2019. From 2016 to 2019, he was a Research Fellow with the Information and Communications Engineering Group, University College London. He joined UCL from the High-Performance Networks Group, University of Bristol, where he was a Senior Research Associate. He is currently the Associate Editor of *Frontiers in Communications and Networks, IET Electronics Letters* and a Section Editor of MDPI Sensors *Communications*. From 2010 to 2011, he held the prestigious Marie Curie Fellowship at the European Organization for Nuclear Research (CERN).

ZABIH GHASSEMLOOY (Senior Member, IEEE) received the B.Sc. (Hons.) degree in electrical and electronics engineering from Manchester Metropolitan University, U.K., in 1981, and the M.Sc. and Ph.D. degrees from the University of Manchester, U.K., 1984 and 1987, respectively. From 1987 to 1988, he was a Postdoctoral Research Fellow with the City University, U.K. In 1988, he joined Sheffield Hallam University as a Lecturer, becoming a Professor, in 1997. In 2004, he joined the University of Northumbria, Newcastle, as an Associate Dean (AD) for research with the School of Engineering, and from 2012 to 2014, he was an AD for Research and Innovation with the Faculty of Engineering and Environment, where he is currently the Head of the Optical Communications Research Group. In 2001, he was awarded Tan Chin Tuan Fellowship in Engineering from Nanyang Technological University, Singapore. In 2016, he was a Research Fellow and, in 2015, a Distinguished Professor with the Chines Academy of Science, Quanzhou, China. He was a Visiting Professor with the University Tun Hussein Onn Malaysia (2013–2017) and Huaqiao University, China (2017–2018). He has published over 880 articles (347 journals and eight books), 100 keynote/invited talks, and supervised 65 Ph.D.' s. He is a coauthor of a CRC book on *Optical Wireless Communications - Systems and Channel Modeling with Matlab* (1st Ed. 2012, and 2nd Ed. 2019), a co-editor of four books including the Springer book on *Optical Wireless Communications - An Emerging Technology (2016)*, CRC book on *Visible Light Communications: Theory and Applications*, (June 2017), IGI Global book on *Intelligent Systems for Optical Networks Design: Advancing Techniques*, (March 2013), and IET book on *Analogue Optical Fiber Communications*, IEE Telecommunication series 32, 1995. His research interests include optical wireless communications, free space optics, visible light communications, radio over fiber- free space optics, and sensor networks with project funding from EU, UK Research Council, and industry. He is a CEng, a Fellow of IET, and a Fellow of OSA. He was the Vice-Chair of EU Cost Action IC1101 (2011–2016). He is the Chief Editor of *British Journal of Applied Science and Technology* and *International Journal of Optics and Applications*, an Associate Editor of a number of international journals, and Co-guest Editor of a number of special issues. He is the Founder and Chair of the IEEE/IET Intern. Symposium on Communications Systems, Networks and DSP, West Asian Colloquium on Optical Wireless Communications, and co-founder of a number of international events including Workshop on Optical Wireless Communications in ICC, since 2015. He has been the Vice-Chair of OSA Technical Group of Optics in Digital Systems (2018-). He has been the Chair of the IEEE Student Branch at Northumbria University, Newcastle (2019-). From 2004 to 2006, he was the IEEE UK/IR Communications Chapter Secretary, the Vice-Chairman (2006–2008), the Chairman (2008–2011), and the Chairman of the IET Northumbria Network (October 2011–2015).

STANISLAV ZVANOVEC (Senior Member, IEEE) received the M.Sc. and Ph.D. degrees from Czech Technical University (CTU) in Prague, in 2002 and 2006, respectively. He is currently a Full Professor, the Deputy Head of the Department of Electromagnetic Field and a Leader of Wireless and Fiber Optics team at CTU. His current research interests include free space optics (FSO) and fiber optical systems, visible light communications (VLC), RF over optics. He is author of two books and more than 250 journal articles and conference papers.